Available online at www.sciencedirect.com
SCIENCE DIRECT®
Journal of Molecular Graphics and Modelling 24 (2005) 72–80
Journal of Molecular Graphics and Modelling
www.elsevier.com/locate/JMGM

Structural model of the *Plasmodium* CDK, Pfmrk, a novel target for malaria therapeutics

Youyi Peng, Susan M. Keenan, William J. Welsh *

Department of Pharmacology, University of Medicine & Dentistry of New Jersey-Robert Wood Johnson Medical School (UMDNJ-RWJMS) and the Informatics Institute of UMDNJ, Piscataway, NJ 08854, USA

Received 10 February 2005; accepted 7 June 2005
Available online 19 July 2005

Abstract

Malaria, with 300–500 million clinical cases resulting in 1–3 million fatalities a year, is one of the most deadly tropical diseases. As current antimalarial therapeutics become increasingly ineffective due to parasitic resistance, there exists an urgent need to develop and pursue new therapeutic strategies. Recent genome sequencing and molecular cloning projects have identified several enzymes from *Plasmodium* (*P.*) *falciparum* that may represent novel drug targets, including a family of proteins that are homologous to the mammalian cyclin-dependent kinases (CDKs). CDKs are essential for the control of the mammalian cell cycle and, based on the conservation of the CDKs across species, the plasmodial CDKs are expected to play a crucial role in parasitic growth. Here we present a 3D structural model of Pfmrk, a putative human CDK activating kinase (CAK) homolog in *P. falciparum.* Notable features of the present structural model include: (1) parameterization of the Mg^{2+} hexacoordination system using ab initio quantum chemical calculations to accurately represent the ATP-kinase interaction; and (2) comparison between the docking scores and measured binding affinities for a series of oxindole-based Pfmrk inhibitors of known activity. Detailed analysis of inhibitor-Pfmrk binding interactions enabled us to identify specific residues (viz. Met66, Met75, Met91, Met94 and Phe143) within the Pfmrk binding pocket that may play an important role in inhibitor binding affinity and selectivity. The availability of this Pfmrk structural model, together with insights gained from analysis of ligand–receptor interactions, should promote the rational design of potent and selective Pfmrk inhibitors as antimalarial therapeutics.

Keywords: *Plasmodium falciparum*; CDK; Pfmrk; Structural model; Homology modelling; Oxindoles; Ligand docking

1. Introduction

Among the four malarial parasites that exploit a human host, *Plasmodium* (*P.*) *falciparum* is the most lethal form and alone responsible for 95% of the 1–3 million deaths resulting from this disease [1,2]. Moreover, increasing drug resistance in the malaria parasites to traditional therapeutics such as chloroquine has led to an alarming resurgence of the disease in the last several decades [3,4]. Although much effort has been dedicated to the study of malaria, until recently, little has been known about the regulatory mechanism of the parasitic life cycle. Prospects have brightened with the genome sequencing and molecular cloning of several kinases from *P. falciparum* that are homologous to the mammalian cyclin-dependent kinases (CDKs) [5–9]. CDKs are a family of protein kinases that control cell cycle progression and, consequently, represent viable targets for drug development [10–14]. *P. falciparum* CDKs, by virtue of their similarity in sequence and structure to the mammalian homologues, have become attractive targets for novel antimalarial therapeutics [15,16].

Pfmrk is a *P. falciparum* kinase isolated in 1996 using a PCR approach. Of the mammalian CDKs, human CDK7 (hCDK7) has the highest sequence identity (46%) to Pfmrk [9]. CDK7 has dual functions: acting as the cyclin-dependent kinase activating kinase (CAK) and when complexed with TFIIH, as a transcription factor to regulate transcription and DNA repair. The prospect that the parasitic kinase Pfmrk exhibits a similar twofold function would

* Corresponding author. Tel.: +1 732 235 3234; fax: +1 732 235 3475.
E-mail address: welshwj@umdnj.edu (W.J. Welsh).

1093-3263/$ – see front matter © 2005 Elsevier Inc. All rights reserved.
doi:10.1016/j.jmgm.2005.06.002

render it a highly attractive target for therapeutic inhibitors. Once expressed in *E. Coli*, Pfmrk kinase activity has been observed against histone H1 [17] and the carboxyl-terminal domain (CTD) of the large subunit of RNA polymerase II [18]. Moreover, association of Pfmrk with human cyclin H (the cyclin partner for hCDK7) [17] or Pfcyc-1 (a cyclin homologue in *P. falciparum*) [19] stimulates kinase activity in vitro. The endogenous cyclin-dependent kinase inhibitor (CDI), $p21^{CIP1}$, inhibits a wide range of CDKs including Pfmrk activity [18]. While this body of data strongly supports the notion that Pfmrk is a parasitic CDK homologue, recent publications have suggested that Pfmrk may represent a unique family of protein kinases [20,21]. Thus far, CAK activity by Pfmrk has not been detected in vitro against PfPK5 or other CDK-related kinases [19]. In addition to the binding of cyclin, the full activation of CDK7 requires the association of an assembly factor, Mat1 [22,23]. Whether Pfmrk does indeed function as a CAK but requires one or more accessory elements (such as a Mat1 functional homolog) for activity or has a discrete function in the parasite remains to be determined.

In this paper, a structural model of Pfmrk was constructed using homology modeling techniques. Parameterization of the Mg^{2+} hexacoordinate system as found in the hCDK2 was achieved using ab initio quantum chemical calculations in order to represent the Mg^{2+}–ATP–protein interaction. The partial atomic charges so obtained were imported into the Pfmrk homology model, and structural refinement using energy minimization and molecular dynamics simulations followed. To assess the validity of the Pfmrk structural model, a series of known 1,3-dihydro-indol-2-ones (henceforth described as oxindoles) Pfmrk inhibitors were docked and scored for subsequent comparison with the measured inhibitory activity of these compounds. Detailed analysis of inhibitor–Pfmrk interactions identified residues deemed responsible for the binding affinity and selectivity of these oxindoles for Pfmrk over the human CDKs. This information is extremely useful for guiding the rational design of safe and effective inhibitors of Pfmrk as potential antimalarial therapeutics.

2. Methods

All calculations were conducted on SGI Octane R12000 machines. Development of the Pfmrk structural model proceeded in five steps: sequence analysis, ab initio parameterization, homology modeling, energy minimization (EM) and molecular dynamics (MD) simulations, and inhibitor docking and scoring. The procedures employed for each step are described below.

2.1. Sequence analysis

All sequence data were obtained from the National Center for Biotechnology Information (NCBI, http://www.ncbi.nlm.nih.gov/) The accession numbers of Pfmrk and human CDK2 (hCDK2) are AAD55782 and P24941, respectively. Multiple sequence alignments for a series of CDKs, as well as pairwise alignment (Fig. 1) between hCDK2 and Pfmrk, were conducted using the ClustalW1.8 routine with default parameters [24,25]. The alignment revealed one 5-residue and one 13-residue insertions in Pfmrk. To predict the secondary structure for these two inserted regions, the Pfmrk sequence was submitted to a secondary structure prediction server (http://cubic.bioc.columbia.edu/pp/submit_meta.html) having access to six prediction algorithms: PHD, [26] PROF, [27] PSIPRED, [28] PSSP, [29] SSPRO, [30] and SAM-T99 [31]. In addition, the sequence for the larger insertion (residues from Y163 to Y175 in Pfmrk) was submitted to BLAST (http://ncbi.nlm.nih.gov/blast) [32] to search for short nearly exact matches.

Fig. 1. Sequence alignment of hCDK2 and Pfmrk with ClustalW 1.8. Residues that are identical between the two sequences are shaded with a black background, while similar residues are shaded with a gray background. The gaps are indicated with (−). The numbering refers to Pfmrk.

2.2. Homology modeling

The active crystal structure of hCDK2 (pdb ID = 1QMZ) [33] was chosen as the template for the homology modeling of Pfmrk. The template structure was retrieved from the Research Collaboratory for Structural Bioinformatics Protein Data Bank (http://www.rcsb.org/pdb) [34] and submitted to the WHATIF server for structural verification (http://www.cmbi.kun.nl/gv/servers/WIWWWI/) [35]. The initial homology model was constructed using the InsightII 2000 software package (http://www.accelrys.com) [36]. The structurally conserved regions (SCRs) between hCDK2 and Pfmrk were identified based on sequence and functional similarity. The 3D coordinates within SCRs were copied from the template hCDK2 to Pfmrk. De novo loop generation was employed to yield the coordinates for variable regions (VRs) which consisted of loop regions not contained within the SCRs. The inclusion of randomly modeled regions required splice-site relaxation to allow the protein backbone to adopt appropriate psi/phi angles. This procedure was performed by relaxing the backbone atoms of the residues involved in the splice sites. The side chains of the Pfmrk structural model were checked for acceptable position of rotatable bonds and absence of severe steric overlaps by using the internal rotamer library in InsightII. In existing CDK structures, a bivalent cation (Mg^{2+}) and a water molecule have been observed to aid in the coordination between the phosphate groups of ATP and binding site residues [33]. Therefore, the ATP, Mg^{2+} ion, and associated water molecule were extracted from the hCDK2 structure and manually positioned into the preliminary Pfmrk model. Following resolution of steric clashes, this protein–Mg^{2+}–ATP complex was solvated in water and submitted to EM and MD simulations (details below) to refine the Pfmrk structural model.

2.3. Ab initio parameterization

The EM and MD refinement procedures of the Pfmrk-ATP structural model required parameterization of the Mg^{2+} ion within its hexacoordinate environment: atomic charges, van der Waals radius and force constant for nonbonded interactions. Using inactive conformations of hCDK2 and human CDK1 (hCDK1) as the structural models, Cavalli et al. have previously demonstrated that ab initio parameterization of a CDK active site using restrained electrostatic potential (RESP) fit techniques is a practical strategy that lends itself to the study of other CDKs [37]. In the active conformation of hCDK2, the Mg^{2+} ion forms a hexacoordinate octahedral complex with the side chains of Asn132 and Asp145, the oxygen atoms of the ATP triphosphate group, and one water molecule (Fig. 2). In addition, the protonated side chain of Lys33 proximal to the α-phosphate O atom will likely influence electrostatic interactions on the Mg^{2+} coordination system [37]. These three residues are conserved across the mammalian and parasitic CDKs, making it reasonable to assume that the Mg^{2+} coordination system is conserved in Pfmrk. As such, the model system for our quantum mechanical calculations comprised the residues Asn132, Asp145 and Lys33, ATP, the Mg^{2+} ion and one water molecule extracted from the 1QMZ structure. To decrease the computational burden, all residues and ATP were truncated to representative model species: acetamide for Asn132; acetate ion for Asp145; methylammonium for Lys33; and methyltriphosphate for ATP [37]. The geometry of the Mg^{2+} coordination system was extracted from the hCDK2 crystal structure (1QMZ). Hydrogen atoms were then added where the amino acids and ATP were truncated.

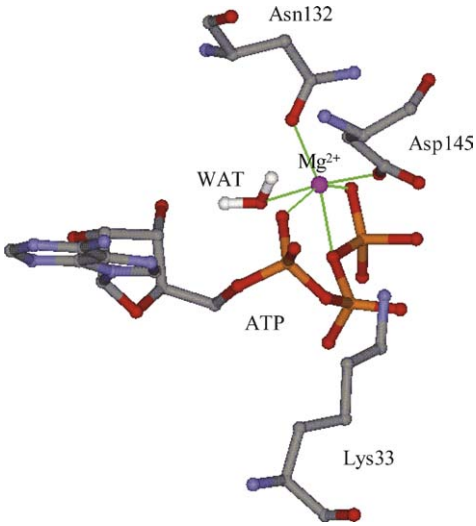

Fig. 2. The Mg^{2+} hexacoordinate system. The protein residues and ATP are displayed as ball and stick and colored by atom-type. The Mg^{2+} ion is colored magenta. The hexacoordinate system is indicated by solid green lines.

The RHF (spin-restricted Hartree-Fock) Hamiltonian with the 6-31G* basis set implemented in the Gaussian 98 package [38] was employed to calculate the electrostatic potential (ESP) for the Mg^{2+} coordination complex. The formal net charge of the complex was constrained to −2.0e, corresponding to the sum of formal charges of the Mg^{2+} ion (+2e), the ATP (−4e), the Lys side chain (+1e), and the Asp side chain (−1e). The atomic charges for the entire coordination system were calculated by means of RESP fit procedure [39] accessed in the AMBER7 package [37]. The AMBER force field was supplemented by these calculated charges for the EM and MD procedures. The van der Waals radius (1.17 Å) and 12-6 Lennard-Jones constant (0.1 kcal/mol) for Mg^{2+} were taken from related studies [37].

2.4. Energy minimization (EM) and molecular dynamics (MD) simulations

Refinement of the Pfmrk structural model was conducted by EM and MD calculations using AMBER7 supplemented by the Mg^{2+}-related parameters described above. In order to

assess if the newly developed parameters are able to preserve the 3D structures of CDKs, MD simulations were first run on the hCDK2 crystal structure (1QMZ). The A chain, ATP, Mg^{2+} and the water molecule associated with the Mg^{2+} hexacoordinate system were extracted from the 1QMZ structure and solvated by a 9 Å radius shell of TIP3 water molecules [40]. The solvated system was energy minimized in two phases: first, 1000 iterations of constrained steepest descent (SD) whereby only the water molecules were free to move to eliminate bad contacts; second, 5000 iterations of SD and 5000 iterations of conjugated gradient (CG) minimization was conducted on the entire system. MD simulations were then run on the resulting system using the standard force-field parameter set *parm99* in AMBER7 with dielectric constant $\varepsilon = 1$ and cutoff distance = 9.0 Å applied for both electrostatic and vdW interactions. The SHAKE algorithm [40] was implemented for bonds involving hydrogen atoms and the time step = 2 fs. The system was coupled to a Berendsen bath at 300 K by using a coupling constant $\tau_T = 2$ ps [41]. The temperature was gradually increased from 100 to 300 K over 10 ps of simulation time with the volume held constant (ensemble NVT). After the temperature was close to 300 K and the density was near 1.0 g/ml, constant pressure and temperature controls (NPT) were applied to the system and the simulation was conducted for 1 ns. The pressure of the system was raised to 1 atm (ensemble NPT). Following precedent [42] employed in similar studies of metallo-protein complexes, distance constraints with harmonic constraints set to 100 kcal/mol were imposed on the Mg^{2+} coordination complex to their experimental values during the MD simulation.

After validation on the hCDK2 system, the force-field parameters were then employed for EM and MD simulations of the ATP-Pfmrk system with the same protocol as for hCDK2. Pfmrk structures derived from the final 400 ps (subsequent to system equilibrium) were averaged and energy minimized using 1000 iterations of SD and 4000 iterations of CG. The geometry of these energy minimized structures was analyzed with PROCHECK [43,44].

2.5. Inhibitor docking and scoring

A series of oxindole-based Pfmrk inhibitors [45,46] were docked to the structural model of Pfmrk using GOLD (Genetic Optimization of Ligand Docking) [47]. The structures and apparent inhibition constants (IC_{50}) of these Pfmrk inhibitors are shown in Table 2. All structures were built with Sybyl 6.8 (http://www.tripos.com) [48] and optimized with the MMFF94 force field and atomic charges. During docking, the default algorithm speed was selected, and the number of poses for each inhibitor was set to 25. The ligand binding site was defined as Pfmrk residues within a 15 Å radius of the centroid of the ATP-purine ring. Early termination was allowed if the RMSD of the top five bound conformations of a ligand were within 1.5 Å. After docking, the 25 individual binding poses of each ligand were re-ranked according to the modified GOLD score (details in text). The top-ranked conformation of each ligand was selected and the corresponding GOLD score was then correlated with the known inhibition constants pIC_{50} ($-\log IC_{50}$). The binding conformations of inhibitors in the ATP-binding site were displayed in DSviewerPro 5.0 (http://www.accelrys.com) [49].

3. Results and discussion

Pfmrk, a kinase from *P. falciparum*, has been identified as a novel target for antimalarial drug discovery by virtue of its homology to the family of CDKs. De novo drug design is significantly enhanced by the availability of 3D coordinates for the target protein. While no high resolution experimental structure exists for Pfmrk, the prospects for developing a high quality structural model are enhanced by the degree of sequence similarity and conservation of functional motifs with potential structural templates. The availability of a structural model for the scientific community would accelerate the rational design of clinically significant inhibitors against this parasitic kinase.

3.1. Sequence analysis and template identification

The identification of a template structure is an essential first step in any homology modeling project. As the active conformation of a kinase is potentially less tolerant of mutations able to preserve kinase function while inducing inhibitor resistance, we sought only active structures as templates for the present purpose. Many of the CDK structures (including PfPK5 [50] and recently resolved hCDK7 [51] structures) represent inactive conformations of the kinases. Fortunately, all CDKs for which high-resolution structural data are available exhibit a highly conserved bilobate fold. Furthermore, the parasitic kinase structures (i.e., PfPK5) add credence to the hypothesis that the fold and inactivation mechanism of the CDKs are highly conserved across evolution. We chose an active (Thr160 phosphorylated) structure of hCDK2 complexed with cyclin A and ATP (pdb ID = 1QMZ) as the template for our Pfmrk model. A WHATIF check of chain A of the 1QMZ template structure suggested minor structural modifications [35]. Specifically, the side chains of ASN3 and HIS119 were flipped 180° to improve the orientation of hydrogen bonding interactions.

In order to identify functionally and structurally conserved regions across the family of CDKs, multiple sequence alignment was performed between the Pfmrk sequence and the sequences of human CDKs 1–9 and PfPK5. This procedure successfully located all major regions that are specific to CDKs are preserved in Pfmrk, including the following notable motifs: (1) the PSTAIRE (single amino acid representation) motif, which is important for cyclin binding and characteristic of all CDKs; (2) residues 80–84 in hCDK2, which have been shown as

essential in the binding of ATP and CDK inhibitors; (3) the phosphorylation site Thr160 in hCDK2; and (4) the GDSEIDQ motif, which is involved in the control of phosphorylation of the activating site and the binding of cyclins [9].

The multiple alignments were followed by pairwise sequence alignment between Pfmrk and the template hCDK2 and, as expected, functionally important motifs are well conserved (Fig. 1). The alignment generates two deletions of one and two residues, and two insertions of five and thirteen residues (Fig. 1) respectively. While the deletions can be easily accommodated within loop regions, modeling of the inserted residues required more attention. Secondary structure predictions from six methods indicated low propensity of these insertion regions for α-helix or β-strand. Furthermore, a BLAST [32] search found no sequences with known secondary structure of high similarity to the 13 residues. Taken together, it is reasonable to assume that the insertions of 5 and 13 residues are each located in loop regions.

3.2. Ab initio parameterization

The ATP-binding pockets of CDKs are located at the cleft between the N and C terminal lobes of the kinase. As known CDK inhibitors are competitive with ATP, it is essential that we correctly simulate the ATP-kinase environment during the refinement process, which entails the parameterization of the Mg^{2+} coordination system. This was completed by performing ab initio quantum mechanical calculations and RESP fit techniques. Comparison of the atomic charges of the Mg^{2+}-amino acid model system derived from the ab initio calculations and the AMBER7 force field (Table 1) reveal that the +2 formal charge of the Mg^{2+} ion is essentially negated by the negative charge of the ATP triphosphate group. Moreover the atomic charges of the amino acid side chains involved in the Mg^{2+} ion coordination system remain similar to those standardized by the AMBER7 force field (Table 1).

3.3. MD simulations

MD simulations (see Section 2) on the hCDK2 structure assured confidence in the parameterization described above, as evidenced by the rapid convergence of the root mean square deviation (R.M.S.D.) of the α-carbon backbone of the sampled conformation starting from hCDK2 initial conformation (Fig. 3, lower curve). After validation of the hCDK2 system, MD simulations on the Pfmrk structural model followed by similar RMSD analysis again indicated a stable 3D structure (Fig. 3, upper curve). PROCHECK [43,44] assessment of the energy-minimized average structure indicated acceptable quality (overall G-factor = −0.3; 1.8% of residues in ''disallowed'' or ''generously disallowed'' regions of the Ramachandran plot). Indeed, all five residues falling outside of the ''allowed'' regions are located either within loop structures or the C-terminal domain.

Table 1
Comparison of calculated RESP charges with standard AMBER charges for the atoms involved in Mg^{2+} coordination system[a]

Residue	Atom	Calculated RESP charges	Standard AMBER charges
Asn132	C	0.99	0.71
Asn132	***O***	***−0.65***	***−0.59***
Asn132	N	−1.06	−0.92
Asn132	H	0.43	0.42
Asn132	H	0.54	0.42
Asp145	C	1.10	0.80
Asp145	O	−0.83	−0.80
Asp145	***O***	***−0.84***	***−0.80***
Lys33	N	−0.21	−0.39
Lys33	H	0.33	0.34
Lys33	H	0.29	0.34
Lys33	H	0.28	0.34
WAT	H	0.34	0.42
WAT	***O***	***−0.75***	***−0.83***
WAT	H	0.42	0.42
Mg^{2+}	Mg	1.00	2.00 (formal)
ATP	Oγ3	−0.86	−0.95
ATP	Pγ	1.20	1.26
ATP	***Oγ1***	***−0.84***	***−0.95***
ATP	Oγ2	−0.89	−0.95
ATP	***Oβ3***	***−0.35***	***−0.53***
ATP	Pβ	1.22	1.39
ATP	Oβ1	−0.86	−0.89
ATP	Oβ2	−0.74	−0.89
ATP	Oα3	−0.51	−0.57
ATP	Pα	1.28	1.25
ATP	Oα1	−0.80	−0.88
ATP	***Oα2***	***−0.83***	***−0.88***

[a] Atoms directly coordinated by Mg^{2+} are shown in bold and italics.

3.4. Evaluation of the Pfmrk 3D structural model

In silico molecular docking and scoring of ligands were conducted to assess the suitability of our Pfmrk model for structure-based drug design. To explore potential ligand-binding conformations and to satisfy ligand-binding requirements we used the docking and scoring algorithms implemented in GOLD [47]. GOLD utilizes a genetic algorithm and takes into account not only full ligand flexibility, but also partial protein flexibility. Specifically, the OH groups of Ser, Thr and Tyr, and the NH_3^+ of Lys residues within the protein active site are allowed to rotate to increase the likelihood of formation of ligand-protein hydrogen bonds. GOLD has been fully validated and is highly regarded for its accuracy and reliability [47,52–54]. While GOLD does produce accurate prediction of ligand binding conformation within a binding pocket, the GOLD scoring function (i.e., GOLD fitness) is not parameterized for small molecule binding affinities. Recently, Verdonk and co-workers [52] reported a modified GOLD scoring function (GOLD score) equal to the GOLD fitness minus the ligand intramolecular terms. The GOLD score has been shown in other systems to provide an improved correlation with experimental binding affinity. Indeed, correlation statistics for GOLD score are comparable to those obtained by the

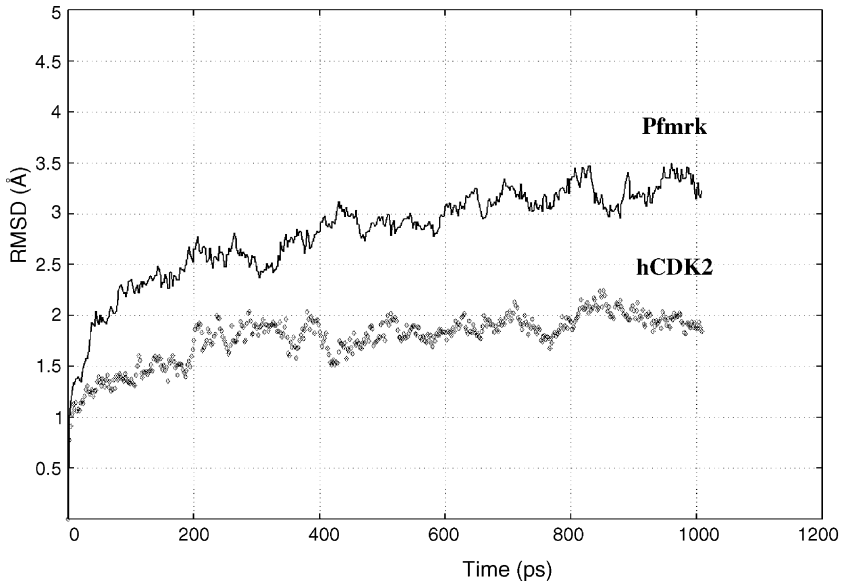

Fig. 3. The α-carbon backbone RMSD of Pfmrk (upper) and hCDK2 (lower) as determined from their respective starting conformations obtained during molecular dynamics simulation.

Chemscore function which was parameterized against experimental binding affinities.

In this study, a series of oxindole-based Pfmrk inhibitors (Table 2) were docked into the refined structural model of Pfmrk. A plot of the GOLD score versus pIC_{50} (Fig. 4) yielded a strong correlation ($r^2 = 0.67$), adding to our confidence in the Pfmrk structural model. All inhibitor molecules used for this study can be ''locked'' into one of two conformations corresponding to E and Z isomers about a double bond (denoted by * in Table 2). Therefore, we compared the results of docking either the E or Z isomers for each inhibitor to Pfmrk. Correlation of the GOLD scores with the pIC_{50} values was much stronger for the E isomers ($r^2 = 0.67$) than for the Z isomers ($r^2 = 0.52$). These results suggest that the E isomers represent the bioactive conformations and indicate a certain degree of structural restraint imposed by the kinase binding site.

The orientations of inhibitors within the Pfmrk binding site determined by this modeling study can provide insights to explain variances in ligand binding affinities for Pfmrk. For clarification, the docked pose of a potent Pfmrk inhibitor, GW5074, [45] in the E conformation (Table 2) is shown in Fig. 5. The N and O atoms of the lactam amide of GW5074 form hydrogen bonds with both the backbone carbonyl and NH groups of Met94. As all known CDK inhibitors form hydrogen bonds within the linker region of the kinase, the conservation of this hydrogen bonding pattern was expected. In addition, the hydroxyl group of GW5074 forms hydrogen bonds with the side chains of both Lys39 and Asp145. While the hydrogen bonds formed between the linker region residues and the ligand may be

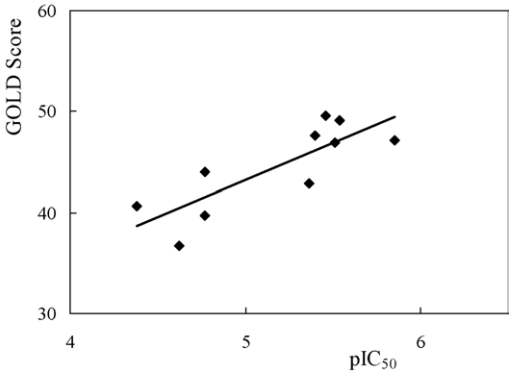

Fig. 4. Correlation of GOLD score and binding affinity (pIC_{50}) for the oxindole-based Pfmrk inhibitors.

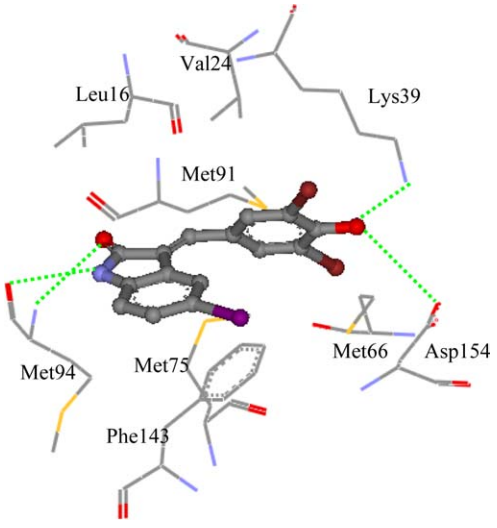

Fig. 5. The binding mode of GW5074 in the ATP-binding pocket of Pfmrk. GW5074 is rendered in ball-and-stick mode and colored by atom-type. The protein residues are rendered in stick mode and also colored by atom-type. The hydrogen bonds are highlighted by dotted green lines.

Table 2
Structures and binding affinities of oxindole-based Pfmrk inhibitors

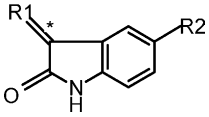

No.	R1	R2	IC_{50} (μM)
1	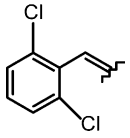	H	17
2	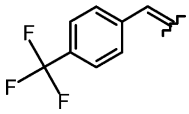	H	4.3
3	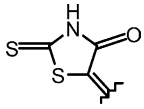	OMe	17.1
4	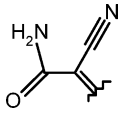	H	24
5	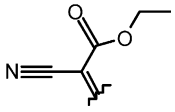	H	41.7
GW5074	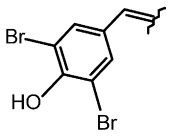	I	~0.5[a]
6	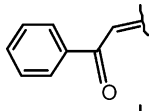	H	4.0
7	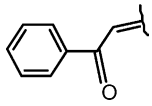	Br	3.1
8	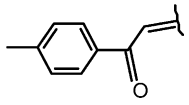	Br	2.9
9	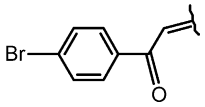	H	3.5
10	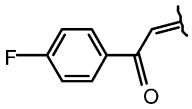	Br	1.4

[a] Private communication [45].

essential for ligand association (and, therefore, for inhibition of the kinase), the hydrogen bonds formed with Lys39 and Asp145 may be responsible for the increase in ligand binding affinity of GW5074 compared with compound #2. In addition, the phenyl ring comprising the side chain of Phe143 interacts with the oxindole ring of the ligand by π–π stacking. The side chains of Met66, Val24 and Met91 also make hydrophobic interactions with the phenyl ring at ligand position R1 (Table 2), while the side chains of Leu16 and Met75 interact via hydrophobic interactions with the oxindole ring. Interestingly, many of the residues involved in hydrophobic interactions (Met66, Met75, Met91 and Phe143) are unique to Pfmrk while those involved in hydrogen bond formation are well conserved. It is highly conceivable that these hydrophobic interactions hold the key for the design of potent and selective Pfmrk inhibitors.

4. Summary and conclusions

A 3D structural model of Pfmrk was constructed and refined using systematic implementation of various computational techniques, including homology modeling, ab initio quantum mechanical calculations, and EM and MD simulations. The refined structural model was further evaluated by the molecular docking of a series of known Pfmrk inhibitors. The strong correlation ($r^2 = 0.67$) between the GOLD scores and inhibition constants (pIC_{50}) adds confidence in the accuracy of the Pfmrk structural model. Visual analysis of inhibitor-protein interactions within the putative binding pocket of Pfmrk identified specific residues (viz. Met66, Met75, Met91, Met94 and Phe143) that may play an important role in ligand binding affinity and selectivity.

We are currently employing the present Pfmrk structural model for the structure-based design of Pfmrk inhibitors as potential anti-malarial therapeutic agents. Thus far, we have identified several novel compounds that exhibit in vitro inhibitory activity against Pfmrk. Importantly, the chemical scaffolds of these inhibitors are distinct from those associated with known CDK inhibitors. We are now pursuing structural optimization of these initial ‘‘hits’’ to obtain higher binding affinity and selectivity for Pfmrk.

Acknowledgments

The authors are grateful to Maj. N.C. Waters, Ph.D., and Capt. J.A. Geyer, Ph.D., of the Division of Experimental Therapeutics at Walter Reed Army Institute of Research (Silver Spring, MD) and to William A. Clark, Ph.D., and Thomas B. Lavoie, Ph.D., of PBL Therapeutics (Piscataway, NJ) for their valuable contributions. Funding for this research was provided by the New Jersey Commission on High Education, the Informatics Institute of the University of Medicine and Dentistry of New Jersey, and the U.S. Army Small Business Innovation Research (SBIR) program contract W81XWH-04-C-0024. The Pfmrk homology model is available upon request to the authors (welshwj@umdnj.edu).

References

[1] J.G. Breman, The ears of the hippopotamus: manifestations, determinants, and estimates of the malaria burden, Am. J. Trop. Med. Hyg. 64 (2001) 1–11.

[2] N.S. Gray, L. Wodicka, A.M. Thunnissen, T.C. Norman, S. Kwon, F.H. Espinoza, D.O. Morgan, G. Barnes, S. LeClerc, L. Meijer, S.H. Kim, D.J. Lockhart, P.G. Schultz, Exploiting chemical libraries, structure, and genomics in the search for kinase inhibitors, Science 281 (1998) 533–538.

[3] P.B. Bloland, E.M. Lackritz, P.N. Kazembe, J.B. Were, R. Steketee, C.C. Campbell, Beyond chloroquine: implications of drug resistance for evaluating malaria therapy efficacy and treatment policy in Africa, J. Infect. Dis. 167 (1993) 932–937.

[4] J. Sachs, P. Malaney, The economic and social burden of malaria, Nature 415 (2002) 680–685.

[5] A. Naderi, A.A. Ahmed, N.L. Barbosa-Morais, S. Aparicio, J.D. Brenton, C. Caldas, Expression microarray reproducibility is improved by optimising purification steps in RNA amplification and labelling, BMC Genomics 5 (2004) 9.

[6] P.B. Ross-Macdonald, R. Graeser, B. Kappes, R. Franklin, D.H. Williamson, Isolation and expression of a gene specifying a cdc2-like protein kinase from the human malaria parasite *Plasmodium falciparum*, Eur. J. Biochem. 220 (1994) 693–701.

[7] V. Bracchi-Ricard, S. Barik, C. Delvecchio, C. Doerig, R. Chakrabarti, D. Chakrabarti, PfPK6, a novel cyclin-dependent kinase/mitogen-activated protein kinase-related protein kinase from *Plasmodium falciparum*, Biochem. J. 347 (Pt 1) (2000) 255–263.

[8] C. Doerig, J. Endicott, D. Chakrabarti, Cyclin-dependent kinase homologues of *Plasmodium falciparum*, Int. J. Parasitol. 32 (2002) 1575–1585.

[9] J.L. Li, K.J. Robson, J.L. Chen, G.A. Targett, D.A. Baker, Pfmrk, a MO15-related protein kinase from Plasmodium falciparum. Gene cloning, sequence, stage-specific expression and chromosome localization, Eur. J. Biochem. 241 (1996) 805–813.

[10] S. Zhai, A.M. Senderowicz, E.A. Sausville, W.D. Figg, Flavopiridol, a novel cyclin-dependent kinase inhibitor, in clinical development, Ann. Pharmacother. 36 (2002) 905–911.

[11] S.H. Chao, D.H. Price, Flavopiridol inactivates P-TEFb and blocks most RNA polymerase II transcription in vivo, J. Biol. Chem. 276 (2001) 31793–31799.

[12] S. Leclerc, M. Garnier, R. Hoessel, D. Marko, J.A. Bibb, G.L. Snyder, P. Greengard, J. Biernat, Y.Z. Wu, E.M. Mandelkow, G. Eisenbrand, L. Meijer, Indirubins inhibit glycogen synthase kinase-3 beta and CDK5/p25, two protein kinases involved in abnormal tau phosphorylation in Alzheimer's disease. A property common to most cyclin-dependent kinase inhibitors? J. Biol. Chem. 276 (2001) 251–260.

[13] A.M. Senderowicz, E.A. Sausville, Preclinical and clinical development of cyclin-dependent kinase modulators, J. Natl. Cancer Inst. 92 (2000) 376–387.

[14] L. Meijer, E. Raymond, Roscovitine and other purines as kinase inhibitors. From starfish oocytes to clinical trials, Acc. Chem. Res. 36 (2003) 417–425.

[15] N.C. Waters, J.A. Geyer, Cyclin-dependent protein kinases as therapeutic drug targets for antimalarial drug development, Expert Opin. Ther. Targets 7 (2003) 7–17.

[16] C. Doerig, Protein kinases as targets for anti-parasitic chemotherapy, Biochim. Biophys. Acta 1697 (2004) 155–168.

[17] N.C. Waters, C.L. Woodard, S.T. Prigge, Cyclin H activation and drug susceptibility of the Pfmrk cyclin dependent protein kinase from *Plasmodium falciparum*, Mol. Biochem. Parasitol. 107 (2000) 45–55.

[18] Z. Li, K. Le Roch, J.A. Geyer, C.L. Woodard, S.T. Prigge, J. Koh, C. Doerig, N.C. Waters, Influence of human p16(INK4) and p21(CIP1) on the in vitro activity of recombinant *Plasmodium falciparum* cyclin-dependent protein kinases, Biochem. Biophys. Res. Commun. 288 (2001) 1207–1211.

[19] K. Le Roch, C. Sestier, D. Dorin, N. Waters, B. Kappes, D. Chakrabarti, L. Meijer, C. Doerig, Activation of a Plasmodium falciparum cdc2-related kinase by heterologous p25 and cyclin H. Functional characterization of a *P. falciparum* cyclin homologue, J. Biol. Chem. 275 (2000) 8952–8958.

[20] Z. Guo, J.W. Stiller, Comparative genomics of cyclin-dependent kinases suggest co-evolution of the RNAP II C-terminal domain and CTD-directed CDKs, BMC Genomics 5 (2004) 69.

[21] P. Ward, L. Equinet, J. Packer, C. Doerig, Protein kinases of the human malaria parasite *Plasmodium falciparum*: the kinome of a divergent eukaryote, BMC Genomics 5 (2004) 79.

[22] J. Shuttleworth, The regulation and functions of cdk7, Progr. Cell Cycle Res. 1 (1995) 229–240.

[23] H. Serizawa, T.P. Makela, J.W. Conaway, R.C. Conaway, R.A. Weinberg, R.A. Young, Association of Cdk-activating kinase subunits with transcription factor TFIIH, Nature 374 (1995) 280–282.

[24] J.D. Thompson, D.G. Higgins, T.J. Gibson, CLUSTAL W: improving the sensitivity of progressive multiple sequence alignment through sequence weighting, position-specific gap penalties and weight matrix choice, Nucl. Acids Res. 22 (1994) 4673–4680.

[25] R. Lopez, S. Programme, A. Loyd, ClustalW WWW service at the European Bioinformatics Institute, http://www.ebi.ac.uk/clustalw

[26] B. Rost, C. Sander, Prediction of protein secondary structure at better than 70% accuracy, J. Mol. Biol. 232 (1993) 584–599.

[27] J. Park, S.A. Teichmann, T. Hubbard, C. Chothia, Intermediate sequences increase the detection of homology between sequences, J. Mol. Biol. 273 (1997) 349–354.

[28] D.T. Jones, Protein secondary structure prediction based on position-specific scoring matrices, J. Mol. Biol. 292 (1999) 195–202.

[29] G.P.S. Raghava, Protein secondary structure prediction using nearest neighbor and neural network approach, CASP 4 (2000) 75–76.

[30] P. Baldi, S. Brunak, P. Frasconi, G. Soda, G. Pollastri, Exploiting the past and the future in protein secondary structure prediction, Bioinformatics 15 (1999) 937–946.

[31] K. Karplus, C. Barrett, R. Hughey, Hidden Markov models for detecting remote protein homologies, Bioinformatics 14 (1998) 846–856.

[32] S.F. Altschul, T.L. Madden, A.A. Schaffer, J. Zhang, Z. Zhang, W. Miller, D.J. Lipman, Gapped BLAST and PSI-BLAST: a new generation of protein database search programs, Nucl. Acids Res. 25 (1997) 3389–3402.

[33] N.R. Brown, M.E. Noble, J.A. Endicott, L.N. Johnson, The structural basis for specificity of substrate and recruitment peptides for cyclin-dependent kinases, Nat. Cell Biol. 1 (1999) 438–443.

[34] H.M. Berman, J. Westbrook, Z. Feng, G. Gilliland, T.N. Bhat, H. Weissig, I.N. Shindyalov, P.E. Bourne, The Protein Data Bank, Nucl. Acids Res. 28 (2000) 235–242.

[35] G. Vriend, WHAT IF: a molecular modeling and drug design program, J. Mol. Graph 8 (1990) 52–56.

[36] InsightII 2000: Accelrys Inc., San Diego, CA.

[37] A. Cavalli, C. Dezi, G. Folkers, L. Scapozza, M. Recanatini, Three-dimensional model of the cyclin-dependent kinase 1 (CDK1): Ab initio active site parameters for molecular dynamics studies of CDKs, Proteins 45 (2001) 478–485.

[38] M.J. Frisch, G.W Trucks, H.B. Schlegel, G.E. Scuseria, M.A. Robb, J.R. Cheeseman, J.A. Montgomery, Jr., T. Vreven, K.N. Kudin, J.C. Burant, J. M. Millam, S.S. Iyengar, J. Tomasi, V. Barone, B. Mennucci, M. Cossi, G. Scalmani, N. Rega, G.A. Petersson, H. Nakatsuji, M. Hada, M. Ehara, K. Toyota, R. Fukuda, J. Hasegawa, M. Ishida, T. Nakajima, Y. Honda, O. Kitao, H. Nakai, M. Klene, X. Li, J.E. Knox, H.P. Hratchian, J.B. Cross, C. Adamo, J. Jaramillo, R. Gomperts, R.E. Stratmann, O. Yazyev, A.J. Austin, R. Cammi, C. Pomelli, J.W. Ochterski, P.Y. Ayala, K. Morokuma, G.A. Voth, P. Salvador, J.J. Dannenberg, V.G. Zakrzewski, S. Dapprich, A.D. Daniels, M.C. Strain, O. Farkas, D.K. Malick, A.D. Rabuck, K. Raghavachari, J.B. Foresman, J.V. Ortiz, Q. Cui, A.G. Baboul, S. Clifford, J.

Cioslowski, B.B. Stefanov, G. Liu, A. Liashenko, P. Piskorz, I. Komaromi, R.L. Martin, D.J. Fox, T. Keith, M.A. Al-Laham, C.Y. Peng, A. Nanayakkara, M. Challacombe, P.M.W. Gill, B. Johnson, W. Chen, M.W. Wong, C. Gonzalez, J.A. Pople Gaussian98: Gaussian, Inc., Pittsburgh PA, 1998.

[39] C.I. Bayly, P. Cieplak, W. Cornell, P.A. Kollman, A well-behaved electrostatic potential based method using charge restraints for deriving atomic charges: the RESP model, J. Phys. Chem. 97 (1993) 10269–10280.

[40] J.P. Ryckaert, G. Ciccotti, H.J.C. Berendsen, Numerical integration of Cartesian equation of motion of a system with constraints:molecular dynamics of *N*-alkanes, J. Comput. Phys. 23 (1977) 327–341.

[41] H.J.C. Berendsen, J.P.M. Postm, W.F. Van Gunsteren, A. Di Nola, J.R. Haak, Molecular dynamics with coupling to an external bath, J. Chem. Phys. 81 (1984) 3684–3690.

[42] L. Banci, S. Schroder, P.A. Kollman, Molecular dynamics characterization of the active cavity of carboxypeptidase A and some of its inhibitors adducts, Proteins 4 (1992) 288–305.

[43] A.L. Morris, M.W. MacArthur, E.G. Hutchinson, J.M. Thornton, Stereochemical quality of protein structure coordinates, Proteins 12 (1992) 345–364.

[44] R.A. Laskowski, M.W. MacArthur, D.S. Moss, J.M. Thornton, PROCHECK: a program to check the stereochemical quality of protein structures, J. Appl. Cryst. 26 (1993) 283–291.

[45] N.C. Waters, Personal communication, 2003.

[46] C.L. Woodard, Z. Li, A.K. Kathcart, J. Terrell, L. Gerena, M. Lopez-Sanchez, D.E. Kyle, A.K. Bhattacharjee, D.A. Nichols, W. Ellis, S.T. Prigge, J.A. Geyer, N.C. Waters, Oxindole-based compounds are selective inhibitors of Plasmodium falciparum cyclin dependent protein kinases, J. Med. Chem. 46 (2003) 3877–3882.

[47] G. Jones, P. Willett, R.C. Glen, A.R. Leach, R. Taylor, Development and validation of a genetic algorithm for flexible docking, J. Mol. Biol. 267 (1997) 727–748.

[48] Sybyl 6.8: Tripos, Inc.: St. Louis, MO.

[49] DSviewerPro 5.0: Accelrys Inc., San Diego, CA.

[50] S. Holton, A. Merckx, D. Burgess, C. Doerig, M. Noble, J. Endicott, Structures of *P. falciparum* PfPK5 test the CDK regulation paradigm and suggest mechanisms of small molecule inhibition, Structure 11 (2003) 1329–1337.

[51] G. Lolli, E.D. Lowe, N.R. Brown, L.N. Johnson, The crystal structure of human CDK7 and its protein recognition properties, Structure 12 (2004) 2067–2079.

[52] M.L. Verdonk, J.C. Cole, M.J. Hartshorn, C.W. Murray, R.D. Taylor, Improved protein-ligand docking using GOLD, Proteins 52 (2003) 609–623.

[53] J.W. Nissink, C. Murray, M. Hartshorn, M.L. Verdonk, J.C. Cole, R. Taylor, A new test set for validating predictions of protein-ligand interaction, Proteins 49 (2002) 457–471.

[54] M. Kontoyianni, L.M. McClellan, G.S. Sokol, Evaluation of docking performance: comparative data on docking algorithms, J. Med. Chem. 47 (2004) 558–565.